PULSE-CODING FOR SYNTHETIC APERTURE SONAR

Geoffrey Shippey[1], Jörgen Pihl[2]

[1] Queensferry Consulatnts Ltd., Edinburgh, geoffey.shippey@telia.com
[2] Swedish Defence Research Agency, Stockholm, jorgen.pihl@foi.se

ABSTRACT

Platform speed for SAS operation is limited by ping-rate. There can sometimes be a problem of moving fast enough for hydrodynamic stability. When ping-rate is too high for the sonar frequency, targets in the far field are aliassed into ghost targets at shorter range. This paper investigates aliassing in the absence of any form of pulse coding, showing that both bright pixels and mean power in the aliassed region are attenuated by the SAS operation, as well as by natural attenuation due to spreading loss, propagation loss etc. Further attenuation can be achieved by pulse coding. Two forms of Doppler-tolerant coding are investigated, a) up-down linear chirp waveforms b) complementary waveforms using chirp chips. Results suggest that pulse coding can be used with advantage to optimise operational range and platform speed.

1. INTRODUCTION

Suppression of range ambiguities by pulse coding has received relatively little attention for Synthetic-Aperture Sonar (SAS) compared with radar, and even SAR, eg [1-5]. Although SAS and SAR are in many ways very similar, the long propagation times present a special problem for SAS. The platform must not move more than half the length of the receiver array between pings. Otherwise echoes are undersampled, leading to azimuthal ambiguities in the image [6]. When ping-rate is restricted to a few pulses per second, this can limit platform speed severely.

Ping-rate is usually limited by the need to avoid significant echoes arriving from far range after the following ping has been transmitted. Far range echoes are attenuated by a variety of mechanisms, including spreading loss, absorption in the water column, shallow incidence angle, and the sonar antenna design, but there is always the possibility that a strong target will be aliased into the intended range bracket. Common practice is to set the ping rate so low that any distant aliased echo is likely to be extremely weak. However this means reducing platform speed, which not only reduces the rate of area coverage, but may even prejudice the hydrodynamic stability of the vehicle.

This paper investigates the effect of aliasing on the SAS image, with and without any form of pulse coding. Pulse coding methods include the well-known up-down chirp coding method, as well as other forms of pulse coding developed for radar. The paper consists mainly of simulation studies of a 100 kHz sonar system designed to image targets out to 100 m range. Targets beyond 100m range are aliased down to the 0-100 m range bracket, appearing as a ghost targets in the image. There might be some objection to using a 100 kHz sonar out to a maximum range of only 100 m. However the SAS system is intended for sea-mine identification, and there are operational advantages in using the same frequency range for detection and identification. Nevertheless, for those interested in higher frequency operation, attenuation figures are also given for a sonar operating at 200 kHz centre frequency. Bandwidth was 30 kHz for the 100 kHz system, 60 kHz for the 200 kHz system. Synthetic aperture length was 8m. The simulation used a 32-channel receiver array, but at the chosen platform speed, only 22 channels were used to record each ping. Sampling frequency was 80 kHz for the 100 kHz sonar, and 160 kHz for the 200 kHz sonar.

2. NATURAL ATTENUATION

At a sound speed of 1500 m/sec, the maximum range of 100 m is set by a ping repetition frequency of 7.5 pps. Assume for the moment a uniform scene in terms of seabed reflectivity and reflections from target objects. We will consider reflectors at range *R* in the 100-200 m range, which are aliased down to (*R*–100) m.

This aliased image is attenuated by at least the following mechanisms, compared with an image of the same reflector located at the aliased range:

(a) spreading loss
(b) absorption in the water column due to the additional 200 m round trip path length
(c) attenuation due to elevation beam patterns of transmitter and receiver.

Seabed reverberation is also attenuated by a factor depending on the elevation angle made by the incident wave and echo with the seabed. However this attenuation will not necessarily apply to targets lying on the seabed.

Table 1 below gives the nominal attenuation at 100 kHz of echoes from a point reflector at true range, compared with a point reflector at the aliassed range, 100 m closer to the platform.

Aliassed range	Spreading loss	Absorption loss	Elevation beam-pattern	Total target attenuation	Seabed incidence angle	Total reverberation attenuation
25m	28	7	12	57	24	71
50m	19	7	16	42	12	54
75m	15	7	13	35	5	40
100m	12	7	10	29	0	29

Table 1: Natural Attenuation (dB) versus aliassed range at 100 kHz

Spherical spreading occurs both on transmission to the reflector, and on reflection back to the receiver. An inverse square law is assumed. Absorption losses were calculated for a salinity of 35 psu, pH = 8, and a temperature of 10 degrees. Elevation incidence refers only to seabed reverberation, and assumes that seabed backscatter follows Lambert's Law out to 0.1 radians incidence, after which it remains constant. Hence there is no further attenuation beyond 100 m range as the table shows. The "elevation directivity" is not strictly a natural loss since it depends on the design of the transmitter and receiver elevation beam patterns. Here the sonar is designed to operate between horizontal ranges of 20 m and 100 m, beam depression angle of 26.6 degrees and 5.7 degrees respectively. This gives a nominal beamwidth of 20.8 degrees. Both transmitter and receiver array were tilted 16.1 degrees downwards to 35 m horizontal range from the platform with 6 db points at 20 m and 100 m range. The attenuations assume a sinc beam pattern. At 200 kHz, the figures in Table 1 remain approximately the same, except for an increase in absorption loss to 11 dB.

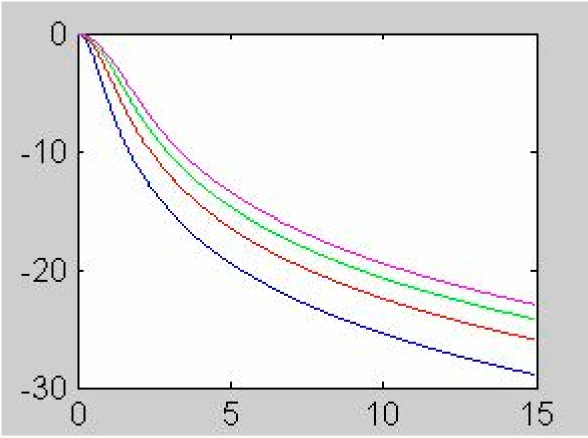

Figure 3.1. Attenuation due to alias defocusing (dB) versus aperture length (metres)
aliassed range: 25m(b), 50m(r) 75m(g), 100m(m)

3. ALIAS ATTENUATION IN SAS IMAGE

We now turn to the characteristics of aliassed targets in the SAS image. Consider a broadside target at range 3*R*, aliassed down to range *R*, and imaged by a Uniform Linear Array (ULA) of length 2*L* using dynamic focus. At each end of the array, the SAS focus algorithm compensates for a range displacement of the echo:

$$\delta r = \sqrt{R^2 + L^2} - R \approx \tfrac{1}{2} L^2 / R \qquad (1)$$

compared with the target range from the ULA centre. True displacement is given by

$$\delta r = \sqrt{9R^2 + L^2} - 3R \approx L^2 / 6R \qquad (2)$$

so the focus error ≈ $L^2/3R$, a little less than the error of ignoring dynamic focus for a true target at range *R*. For SAS, the error can become very large – see Fig 3.1 below. This calculation ignores the window function used to reduce image sidelobes. Window functions reduce image contributions from the aperture ends, where defocusing is greatest.

Fig 3.2 shows the simulated SAS image of a broadside point target aliassed from 150m down to 50 m. The chirp pulse is 1 millisecond long, with centre frequency of 100 kHz and a bandwidth of 50 kHz. Echoes were recorded along an ideal straight synthetic aperture 8 m long, with heading aligned with the track. The intensity of the brightest pixel is 16.3 dB below that of a well-focussed true target at 50 m range, neglecting all the attenuations discussed in Section 2. This corresponds with the graph given in Figure 3.1, after allowing for the Tchebycheff window function.

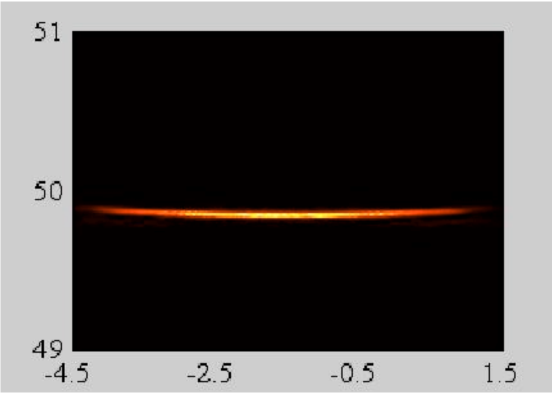

Fig 3.2. Aliassed point target at 150 m true range.

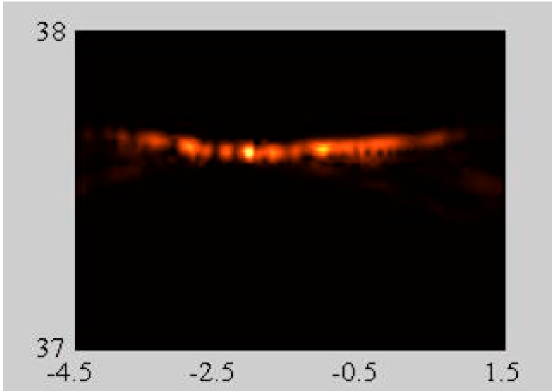

Fig.3.3: Image of similar target from curved track.

If the track is curved, with changing heading, it is less easy to recognize a defocused point target, and peak attenuation is only 12 dB. In Fig 3.3, the defocused point target resembles a rock outcrop.

Attenuations for both uncoded and coded waveforms are summarised in Table 2, giving the attenuation of the brightest pixel in the aliassed image compared with the brightest pixel in a well-focussed SAS image at the unaliassed range. Ideal point targets are used throughout the paper.

The total power in the aliassed image is obtained by summing squared pixel intensities over the whole image. This total power turned out to be the same as that obtained by imaging the same reflector at the aliassed range. Hence aliassing itself introduces no power attenuation in the SAS image.

Aliassed range	100 kHz	200 kHz
25 m	19.7	21.3
50 m	16.1	18.6
75 m	13.7	16.5
100 m	12.2	14.6

Table 2. Brightest Pixel Attenuation (dB) in the Aliassed SAS Image

4. PULSE CODING

4.1 Up/down chirps

One simple scheme is the "up/down chirp". The application of up-down chirp coding to SAR was investigated in [5], which also gives a mathematical analysis of the mismatched signal. It quotes a simulation result of 41.75 dB attenuation for a mismatched 50 :s radar pulse, with bandwidth 135 MHz, compared with the peak value of the correctly matched pulse.

For sonar, Fig 4.1 shows the simulated result when an outgoing up-chirp is match-filtered with the corresponding down-chirp. Using 1 ms pulses with 50 kHz bandwidth gave 25.5 dB attenuation of the mismatched brightest pixel compared with the peak value in the correctly match-filtered image. Attenuation increased to 41 dB using 8 ms chirp pulses (Fig 4.2). Table 3 below summarises the peak intensity attenuations at 100kHz and 200 kHz

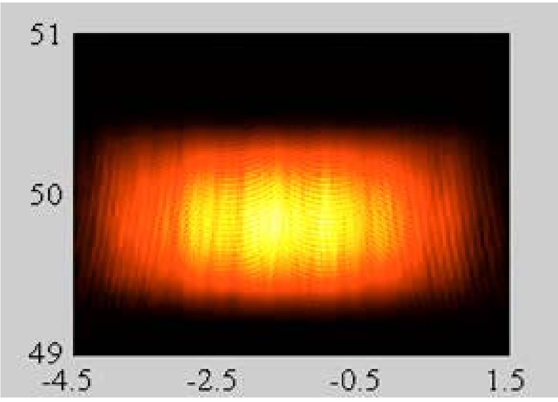

Fig 4.1. Aliassed point target: 1 ms up/down chirp.

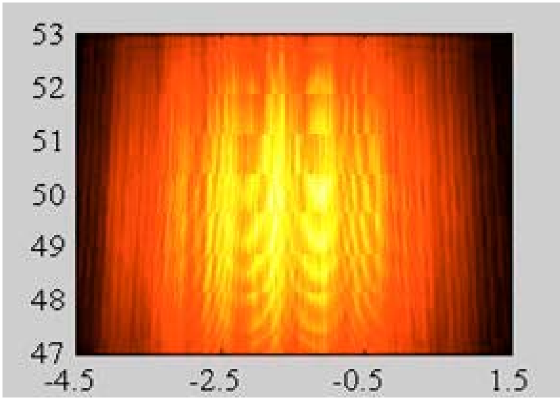

Fig.4.2: Aliassed point target: 8 m/s up/down chirp.

Aliassed range	100 kHz	200 kHz
25 m	39.3	44.0
50 m	36.1	41.1
75 m	33.8	39.3
100 m	32.3	37.4

Table 3. Brightest Pixel Attenuation (dB): 8 ms Up-Down Chirp Coding

Total power in the aliassed coded image is the same as that in the well-focussed image of the same point reflector at the aliassed range. Up-down chirp coding offers no power attenuation.

4.2 Complementary chirp waveforms

The use of complementary waveforms for alias suppression is discussed in [2]. The simplest example is given by the Hadamard Matrix, below left. Frank coding can be used for longer coded sequences [2]. A 4-ping sequence is defined by the 4'th order Frank matrix, below right (MATLAB notation)

```
[1   1                    [1   1   1   1
 1  –1 ]                    1  –j  –1  –j
                            1  –1   1  –1
                            1  –j  –1   j ]
```

Autocorrelation of the coded sequences [1 1] and [1 –1] give [1 2 1] and [-1 2 –1] respectively. If two pulses coded in this way are transmitted alternately, and the match-filtered echoes of point target are precisely synchronized (aligned in time), the auto-correlation functions from two successive pulses sum to [0 1 0]. If the coded sequences are correlated with the previous pulse signature, the outputs are [-1 0 1], [1 0 –1], which sum to [0 0 0]. It is trivial to use these codes to modulate any chosen linear chirp, using the minus sign to invert the waveform. Echoes from an even number of pulses must be summed along the synthetic aperture. The auto-correlation functions of the sequences in the four rows sum to [0 0 0 1 0 0 0], while the ccf 's of each row with a cyclic following row sum to [0 0 0 0 0 0 0]. This Frank code can be used to modulate chirp pulses, representing j by a B/2 phase-shift. The number of pings summed along the synthetic aperture must now be a multiple of 4. Indefinitely long complementary pulse sequences can be generated from higher order Frank matrices.

When used to modulate sonar or radar pulses, the Hadamard or Frank coded echoes must be accurately synchronized in order to achieve the required cancellation properties. The aliassed echoes cannot be correctly aligned if echoes from a true target in the aliased location are well focussed, as discussed in section 3. A similar problem arises with SAR, but there is an important difference. Multi-channel receiver arrays are more common with SAS than with SAR. Using a multi-channel array the platform moves relatively farther between pings, ie between transmission of the complementary waveforms. Hence the misalignment is many times greater.

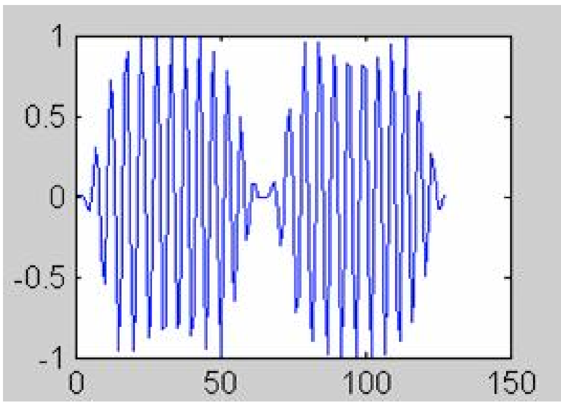

Fig 4.3. Two-chip Hadamard waveform.

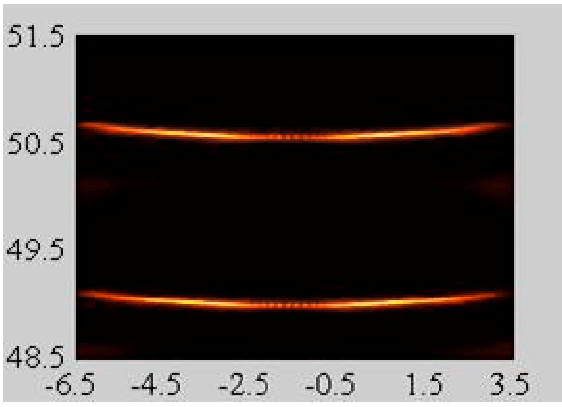

Fig.4.4: Aliassed image using 2-chip Hadamard coding

Simulation studies were carried out at 100 kHz to assess the performance degradation of complementary pulse coding due to time misalignment. In the first study, two 320-sample chips were concatenated to give a 640 sample source signature (Figure 4.3). Figure 4.4 shows a typical aliassed point target image. The target echo in the centre of the frame is precisely cancelled, but the outer components are only partly cancelled leaving two almost identical point-spread functions above and below the aliassed target centre.

Table 4 below gives Brightest Pixel attenuations at the four aliassed ranges, both at 100 kHz and 200 kHz. There is little difference between any of the figures, which average out to about 23 dB. This is much less than attenuations given in Table 3 for up-down chirp coding. However there is now around 5 dB of image power attenuation, showing that aliassed energy is actually cancelled rather than merely smeared out.

Aliassed range	Brightest pixel attenuation (100 kHz)	Image power attenuation (100 kHz)	Brightest pixel attenuation (200 kHz)	Image power attenuation (200 kHz)
25 m	23.4	4.5	25.3	4.4
50 m	23.0	6.2	23.4	4.8
75 m	23.3	5.0	22.3	4.8
100 m	22.2	4.1	22.5	3.9

Table 4: Brightest Pixel and Power Attenuations (dB) using Hadamard-coded Chirps

Further simulations were carried out using 4-chip Frank coding. This gave a few dB more intensity attenuation, but still not enough to compete with up-down chirp coding. Reducing the effective receiver array length from 22 to 6 channels in order to reduce the spacing between transmitter pulses also gave 3 dB additional attenuation. However it makes no sense to shorten the receiver array for pulse coding, since platform speed is first reduced in proportion to array length.

4.3 Autopositioning

The term "autopositioning" covers the use of sonar echoes themselves to correct navigation errors and improve phase-coherence of the SAS image (the usual SAR term is "autofocus") For sonar a common procedure is to correlate echoes from successive pulses using a Displaced Phase Centre Array [7] or otherwise use information derived from individual pings [8]. This presents a problem because range ambiguities are less "smeared out" in azimuth than in the final SAS image. However the up-down chirp coded image is at least smeared out in range.

Complementary waveforms also present problems, because ambiguities are not suppressed in individual echoes, only in consecutive pairs of echoes. Great success has been claimed for Lüke-Schotten codes [4] in the SAR context. Here a long sequence of coded pulses is required to achieve ambiguity suppression, so this form of coding is even less compatible with the autopositioning requirement. Barker and random phase codes [3] also offer orthogonality for individual echoes. Unfortunately these are not Doppler tolerant, which significantly complicates SAS processing.

ATTENUATION COMPARISON

Tables 5a and 5b compare attenuation figures at 100 kHz. The corresponding attenuation figures at 200 kHz are either very similar or higher. It is assumed that for target objects, the most important figure is "brightest pixel attenuation" indicating the intensity of ghost targets in the aliassed image. However for seabed reverberation, it is image power which is more important, indicating the probability of aliassed reverberation weakening the shadow contrast used for target identification.

If up-down chirp coding is used, intensity attenuation ranges from 96 dB at the shortest range to 61 dB at the longest. Power attenuation ranges from 71 dB at the shortest range to 29 dB at the longest. If this is insufficient, it would be possible to sacrifice the last quarter of the range bracket for imaging purposes.

Aliassed range	Uncoded pulses	8 ms up-down chirp	Hadamard 2-chip	Natural Attenuation
25 m	19.6	39.3	25.3	57
50 m	16.3	36.1	23.4	42
75 m	14.1	33.8	22.3	35
100 m	12.3	32.3	22.5	29

Table 5a: Brightest pixel attenuation (dB) at 100 kHz

Aliassed Range	Uncoded pulses	8 ms up-down chirp	Hadamard 2-chip	Natural Attenuation
25 m	0	0	5.0	71
50 m	0	0	6.2	54
75 m	0	0	5.0	40
100 m	0	0	4.1	29

Table 5b: Image power attenuation (dB) at 100 kHz.

5. DISCUSSION

The paper has shown that natural attenuation of the SAS image, combined with up-down chirp coding can give high attenuation of aliased targets and reverberation beyond the nominal maximum range of the sonar. These ideal figures will not always be realised but they strongly suggest that up-down coding should be a standard facility to increase platform speed for a given maximum image range. The performance of Hadamard and Frank coded chirp waveforms was disappointing in conjunction with a long receiver array and wide separation between transmitter pulses. The paper considered other forms of coding which might offer greater attenuation, but these were either Doppler intolerant, or not individually orthogonal, as required for some autopositioning algorithms.

ACKNOWLEDGEMENTS

The first author would like to thank Dr. Marc Pinto of the SACLANT Centre, La Spezia, for useful discussions on this problem.

REFERENCES

[1] Hounam D and Mittermayer J, “Techniques for Reducing SAR Antenna Size”, Proc.*IGARSS*, July 2003, Toulouse.

[2] Kretschmer FF and Gerlach K., “Low sidelobe waveforms derived from orthogonal matrices”, *IEEE Trans. Aerospace and Electronic Systems* **27(1)**, Jan 1991 pp.92-101

[3] Axelson SRJ. ”Suppressed ambiguity in range by phase-coded waveforms”, Proc. *IGARSS*, July 2001, Sydney, **V**, pp.2006-2009.

[4] Krämer G, “Application of Lüke-Schotten codes to SAR interferometry”, Proc. *EUSAR 2000*, Munich, May 2000, pp.483-486.

[5] Mittermayer J. and Marquez J, “Analysis of range ambiguity suppression in SAR by up and down chirp modulation for point and distributed targets”, Proc. *IGARSS* 2003, Toulouse, July 2003, **VI** pp.4077-4079.

[6] Rolt KD and Schmidt H, "Azimuthal ambiguities in synthetic aperture sonar and synthetic aperture radar imagery", *IEEE J.Oceanic Eng.* (Jan.1992), **OE-17** pp.73-79.

[7] Belletini A.and Pinto MA,“Theoretical accuracy of synthetic-aperture sonar micronavigation using a displaced phase-centre array”, *IEEE J. Oceanic Eng.*, **OE-27 (4)**, 2002, pp.780-789.

[8] Shippey G, Pihl J, and Jonsson M, ”Autopositioning for wideband synthetic-aperture sonar using Fast-Factorised Back Projection”, Proc CAD/CAC Conf, Halifax Nov 2002.